axioms

MDPI

Article

Nonlinear Dynamic Behaviors of the (3+1)-Dimensional B-Type Kadomtsev—Petviashvili Equation in Fluid Mechanics

Kang-Jia Wang *, Jing-Hua Liu, Jing Si and Guo-Dong Wang

School of Physics and Electronic Information Engineering, Henan Polytechnic University, Jiaozuo 454003, China
* Correspondence: kangjiaw@hpu.edu.cn

Abstract: This paper provides an investigation on nonlinear dynamic behaviors of the (3+1)-dimensional B-type Kadomtsev—Petviashvili equation, which is used to model the propagation of weakly dispersive waves in a fluid. With the help of the Cole—Hopf transform, the Hirota bilinear equation is established, then the symbolic computation with the ansatz function schemes is employed to search for the diverse exact solutions. Some new results such as the multi-wave complexiton, multi-wave, and periodic lump solutions are found. Furthermore, the abundant traveling wave solutions such as the dark wave, bright-dark wave, and singular periodic wave solutions are also constructed by applying the sub-equation method. Finally, the nonlinear dynamic behaviors of the solutions are presented through the 3-D plots, 2-D contours, and 2-D curves and their corresponding physical characteristics are also elaborated. To our knowledge, the obtained solutions in this work are all new, which are not reported elsewhere. The methods applied in this study can be used to investigate the other PDEs arising in physics.

Keywords: Hirota bilinear equation; periodic-lump solution; multi-wave complexiton solution; multi-wave solution; sub-equation method; traveling wave solutions

MSC: 35C07; 35A22

check for updates

Citation: Wang, K.-J.; Liu, J.-H.; Si, J.; Wang, G.-D. Nonlinear Dynamic Behaviors of the (3+1)-Dimensional B-Type Kadomtsev—Petviashvili Equation in Fluid Mechanics. *Axioms* **2023**, *12*, 95. https://doi.org/10.3390/axioms12010095

Academic Editors: Delfim F. M. Torres and Irina Papkova

Received: 29 November 2022
Revised: 29 December 2022
Accepted: 10 January 2023
Published: 16 January 2023

1. Introduction

Nonlinear partial differential equations (NPDEs) are powerful tools to model various complex phenomena in nature [1–6]. How to obtain the exact solution of the NPDEs has always been the purpose of researchers. To this day, some effective methods have been proposed to seek for the exact solution of the NPDEs such as the Bäcklund transformation method [7–10], Cole—Hopf transformation method [11–14], variational method [15,16], extended rational sine—cosine and sinh—cosh methods [17,18], Sardar subequation method [19,20], the Kudryashov approach [21,22], extended sinh—Gordon equation expansion method [23,24], trial equation method [25,26], sub-equation method [27–29], Wang's direct mapping method [30], and so on [31–35]. In this work, we aim to study the (3+1)-dimensional B-type Kadomtsev—Petviashvili equation that reads as [36]:

$$\psi_{ty} - \psi_{xxxy} - 3\left(\psi_x \psi_y\right)_x + 3\psi_{xz} = 0, \tag{1}$$

Equation (1) is a subclass of the Kadomtsev—Petviashvili (KP) hierarchy and is used to describe the weakly dispersive waves in a fluid. $\psi = \psi(x, y, z, t)$ represents the amplitude or elevation of the relevant wave and is a real function of space x, y, z, and time t. Up to now, many effective methods have been proposed to deal with Equation (1) and some results have been obtained. In [37], two methods, namely the simplest equation method and multiple exp-function method, are used to construct the exact solutions of Equation (1). In [38], one- and two-soliton solutions of Equation (1) are obtained by using the Bäcklund transformations. In [39], the extended homoclinic test technique is employed to study Equation (1) and some new rational breather solutions are found. In [40], the direct algebraic method is adopted and the interaction solutions among solitons, rational waves, and periodic waves are obtained. In [41], the soliton molecules, asymmetric solitons, and some novel hybrid solutions are attained by using the velocity resonance mechanism and the long wave limit method. In [42], the exp-function method aided with symbolic computation is utilized to seek for the anti-kink solutions. However, to our knowledge, the multi-wave complexiton, multi-wave, and periodic lump have not been studied. In addition, the sub-equation method has not been employed to study Equation (1) either. Thus, the objective of this work is to search for the abundant solutions of Equation (1) by means of the Hirota bilinear method and sub-equation method. The results obtained in this work are expected to extend the solutions of the (3+1)-dimensional B-type Kadomtsev—Petviashvili equation. The structure of this article is arranged as follows. In Section 2, the Hirota bilinear equation is developed via the Cole—Hopf transform and the symbolic computation with the ansatz function schemes is utilized to find the multi-wave complexiton solutions, multi-wave solutions, and periodic lump solutions, respectively. In Section 3, the sub-equation method is applied to seek for the traveling wave solutions. In Section 4, the physical characteristics and numerical results of the solutions are presented via the 3-D plots, 2-D contours, and 2-D curves. Finally, the conclusion is provided in Section 5.

2. Cole—Hopf Transform and the Exact Solutions

For constructing the exact solutions of Equation (1), we use the Cole—Hopf transform as:

$$\psi = 2\ln(g)_x. \tag{2}$$

Applying this transform, we can obtain the bilinear form of Equation (1) as:

$$\left(D_y D_t - D_x^3 D_y + 3D_x D_z\right) g \cdot g = 0. \tag{3}$$

Here, the definition of the operators $D_x^m D_t^n$ is [43–46]:

$$D_x^m D_t^n f \cdot g = \left(\frac{\partial}{\partial x} - \frac{\partial}{\partial x'}\right)^m \left(\frac{\partial}{\partial t} - \frac{\partial}{\partial t'}\right)^n f(x,t) g(x',t')\Big|_{x=x',t=t'}. \tag{4}$$

Additionally, there are:
$D_x(f \cdot g) = f_x g - f g_x,$
$D_x^2(f \cdot g) = f_{xx} g - 2 f_x g_x + f g_{xx},$
$D_x^2(f \cdot f) = 2\left(f_{xx} f - f_x^2\right),$
$D_t D_x(f \cdot g) = f_{tx} g - f_t g_x - f_x g_t + g_{tx} f,$
$\cdots \cdots$

2.1. The Multi-Waves Complexiton Solutions

In order to find the multi-wave complexiton solution, it is assumed that the test function g is:

$$\begin{gathered}
\phi = x + \varepsilon_1 y + \varepsilon_2 z + \varepsilon_3 t, \\
\varphi = x + \varepsilon_4 y + \varepsilon_5 z + \varepsilon_6 t, \\
\gamma = x + \varepsilon_7 y + \varepsilon_8 z + \varepsilon_9 t, \\
g = \Delta_1 e^{\varphi} + \Delta_2 e^{-\varphi} + \Delta_3 \sin(\varphi) + \Delta_4 \sin\mathrm{h}(\gamma),
\end{gathered} \tag{5}$$

where $\varepsilon_i (i = 1, 2, \ldots, 9)$ and $\Delta_i (i = 1, 2, 3, 4)$ are real parameters to be determined later. Substituting Equation (5) into Equation (3) and performing the corresponding adjustments, we have:

Case 1:

$\varepsilon_1 = \frac{3\varepsilon_2}{4-\varepsilon_9},\ \varepsilon_2 = \varepsilon_2,\ \varepsilon_3 = \varepsilon_9,\ \varepsilon_4 = \frac{3\varepsilon_2}{\varepsilon_9-4},\ \varepsilon_5 = \frac{\varepsilon_2(2+\varepsilon_9)}{4-\varepsilon_9},\ \varepsilon_6 = \varepsilon_9 - 2,\ \varepsilon_7 = \frac{3\varepsilon_2}{4-\varepsilon_9},\ \varepsilon_8 = \varepsilon_2,\ \varepsilon_9 = \varepsilon_9,$
$\Delta_1 = \Delta_1,\ \Delta_2 = \Delta_2,\ \Delta_3 = \Delta_3,\ \Delta_4 = \Delta_4.$

where $4 - \varepsilon_9 \neq 0$. Applying the above results into Equation (5), we can obtain the multi-wave complexiton solution through the transformation provided by Equation (2) as:

$$\psi(x,y,z,t) = \frac{2\begin{bmatrix} \Delta_1 e^{x+\frac{3\varepsilon_2}{4-\varepsilon_9}y+\varepsilon_2 z+\varepsilon_9 t} - \Delta_2 e^{-(x+\frac{3\varepsilon_2}{4-\varepsilon_9}y+\varepsilon_2 z+\varepsilon_9 t)} + \Delta_3 \cos\left(x + \frac{3\varepsilon_2}{\varepsilon_9-4}y + \frac{\varepsilon_2(2+\varepsilon_9)}{4-\varepsilon_9}z + (\varepsilon_9 - 2)t\right) \\ +\Delta_4 \cosh\left(x + \frac{3\varepsilon_2}{4-\varepsilon_9}y + \varepsilon_2 z + \varepsilon_9 t\right) \end{bmatrix}}{\begin{bmatrix} \Delta_1 e^{x+\frac{3\varepsilon_2}{4-\varepsilon_9}y+\varepsilon_2 z+\varepsilon_9 t} + \Delta_2 e^{-(x+\frac{3\varepsilon_2}{4-\varepsilon_9}y+\varepsilon_2 z+\varepsilon_9 t)} + \Delta_3 \sin\left(x + \frac{3\varepsilon_2}{\varepsilon_9-4}y + \frac{\varepsilon_2(2+\varepsilon_9)}{4-\varepsilon_9}z + (\varepsilon_9 - 2)t\right) \\ +\Delta_4 \sinh\left(x + \frac{3\varepsilon_2}{4-\varepsilon_9}y + \varepsilon_2 z + \varepsilon_9 t\right) \end{bmatrix}} \tag{6}$$

Case 2:

$\varepsilon_1 = \varepsilon_7,\ \varepsilon_2 = \varepsilon_2,\ \varepsilon_3 = \frac{4\varepsilon_7 - 3\varepsilon_2}{\varepsilon_7},\ \varepsilon_4 = -\varepsilon_7,\ \varepsilon_5 = 2\varepsilon_7 - \varepsilon_2,\ \varepsilon_6 = \frac{2\varepsilon_7 - 3\varepsilon_2}{\varepsilon_7},\ \varepsilon_7 = \varepsilon_7,\ \varepsilon_8 = \varepsilon_2,$
$\varepsilon_9 = \frac{4\varepsilon_7 - 3\varepsilon_2}{\varepsilon_7}, \Delta_1 = \Delta_1,\ \Delta_2 = \Delta_2,\ \Delta_3 = \Delta_3,\ \Delta_4 = \Delta_4.$

Inserting the above results into Equation (5) and using the transformation provided by Equation (2), we can obtain the multi-wave complexiton solution as:

$$\psi(x,y,z,t) = \frac{2\begin{bmatrix} \Delta_1 e^{x+\varepsilon_7 y+\varepsilon_2 z+\frac{4\varepsilon_7-3\varepsilon_2}{\varepsilon_7}t} - \Delta_2 e^{-(x+\varepsilon_7 y+\varepsilon_2 z+\frac{4\varepsilon_7-3\varepsilon_2}{\varepsilon_7}t)} + \Delta_3 \cos\left(x - \varepsilon_7 y + (2\varepsilon_7 - \varepsilon_2)z + \frac{2\varepsilon_7-3\varepsilon_2}{\varepsilon_7}t\right) \\ +\Delta_4 \cosh\left(x + \varepsilon_7 y + \varepsilon_2 z + \frac{4\varepsilon_7-3\varepsilon_2}{\varepsilon_7}t\right) \end{bmatrix}}{\begin{bmatrix} \Delta_1 e^{x+\varepsilon_7 y+\varepsilon_2 z+\frac{4\varepsilon_7-3\varepsilon_2}{\varepsilon_7}t} + \Delta_2 e^{-(x+\varepsilon_7 y+\varepsilon_2 z+\frac{4\varepsilon_7-3\varepsilon_2}{\varepsilon_7}t)} + \Delta_3 \sin\left(x - \varepsilon_7 y + (2\varepsilon_7 - \varepsilon_2)z + \frac{2\varepsilon_7-3\varepsilon_2}{\varepsilon_7}t\right) \\ +\Delta_4 \sinh\left(x + \varepsilon_7 y + \varepsilon_2 z + \frac{4\varepsilon_7-3\varepsilon_2}{\varepsilon_7}t\right) \end{bmatrix}} \tag{7}$$

Case 3:

$\varepsilon_1 = \varepsilon_7,\ \varepsilon_2 = \frac{4\varepsilon_7 - 3\varepsilon_3\varepsilon_7}{3},\ \varepsilon_3 = \varepsilon_3,\ \varepsilon_4 = -\varepsilon_7,\ \varepsilon_5 = \frac{(\varepsilon_3+2)\varepsilon_7}{3},\ \varepsilon_6 = \varepsilon_3 - 2,\ \varepsilon_7 = \varepsilon_7,\ \varepsilon_8 = \frac{4\varepsilon_7 - 3\varepsilon_3\varepsilon_7}{3},$
$\varepsilon_9 = \varepsilon_3,\ \Delta_1 = \Delta_1,\ \Delta_2 = \Delta_2,\ \Delta_3 = \Delta_3,\ \Delta_4 = \Delta_4.$

In the same way, we can obtain the multi-wave complexiton solution as:

$$\psi(x,y,z,t) = \frac{2\begin{bmatrix} \Delta_1 e^{x+\varepsilon_7 y+\frac{4\varepsilon_7-3\varepsilon_3\varepsilon_7}{3}z+\varepsilon_3 t} - \Delta_2 e^{-(x+\varepsilon_7 y+\frac{4\varepsilon_7-3\varepsilon_3\varepsilon_7}{3}z+\varepsilon_3 t)} + \Delta_3 \cos\left(x - \varepsilon_7 y + \frac{(\varepsilon_3+2)\varepsilon_7}{3}z + (\varepsilon_3 - 2)t\right) \\ +\Delta_4 \cosh\left(x + \varepsilon_7 y + \frac{4\varepsilon_7-3\varepsilon_3\varepsilon_7}{3}z + \varepsilon_3 t\right) \end{bmatrix}}{\begin{bmatrix} \Delta_1 e^{x+e\eta y+\frac{4\varepsilon_r-3\varepsilon_2\eta_3}{3}+\hat{s}t} + \Delta_2 e^{-(x+\varepsilon_7 y+\frac{4\varepsilon_7-3\varepsilon_3\varepsilon_7}{3}z+\varepsilon_3 t)} + \Delta_3 \sin\left(x - \varepsilon_7 y + \frac{(\varepsilon_3+2)\varepsilon_7}{3}z + (\varepsilon_3 - 2)t\right) \\ +\Delta_4 \sinh\left(x + \varepsilon_7 y + \frac{4\varepsilon_7-3\varepsilon_3\varepsilon_7}{3}z + \varepsilon_3 t\right) \end{bmatrix}} \tag{8}$$

Case 4:

$\varepsilon_1 = \varepsilon_7,\ \varepsilon_2 = \varepsilon_8,\ \varepsilon_3 = \frac{4\varepsilon_7 - 3\varepsilon_8}{\varepsilon_7},\ \varepsilon_4 = -\varepsilon_7,\ \varepsilon_5 = 2\varepsilon_7 - \varepsilon_8,\ \varepsilon_6 = \frac{2\varepsilon_7 - 3\varepsilon_8}{\varepsilon_7},\ \varepsilon_7 = \varepsilon_7,\ \varepsilon_8 = \varepsilon_8,$
$\varepsilon_9 = \frac{4\varepsilon_7 - 3\varepsilon_8}{\varepsilon_7},\ \Delta_1 = \Delta_1,\ \Delta_2 = \Delta_2,\ \Delta_3 = \Delta_3,\ \Delta_4 = \Delta_4.$

Accordingly, the multi-wave complexiton solution of Equation (1) is attained as:

$$\psi(x,y,z,t) = \frac{2\begin{bmatrix} \Delta_1 e^{x+\varepsilon_7 y+\varepsilon_8 z+\frac{4\varepsilon_7-3\varepsilon_8}{\varepsilon_7}t} - \Delta_2 e^{-(x+\varepsilon_7 y+\varepsilon_8 z+\frac{4\varepsilon_7-3\varepsilon_8}{\varepsilon_7}t)} + \Delta_3 \cos\left(x - \varepsilon_7 y + (2\varepsilon_7 - \varepsilon_8)z + \frac{2\varepsilon_7-3\varepsilon_8}{\varepsilon_7}t\right) \\ +\Delta_4 \cosh\left(x + \varepsilon_7 y + \varepsilon_8 z + \frac{4\varepsilon_7-3\varepsilon_8}{\varepsilon_7}t\right) \end{bmatrix}}{\begin{bmatrix} \Delta_1 e^{x+\varepsilon_7 y+\varepsilon_8 z+\frac{4\varepsilon_7-3\varepsilon_8}{\varepsilon_7}t} + \Delta_2 e^{-(x+\varepsilon_7 y+\varepsilon_8 z+\frac{4\varepsilon_7-3\varepsilon_8}{\varepsilon_7}t)} + \Delta_3 \sin\left(x - \varepsilon_7 y + (2\varepsilon_7 - \varepsilon_8)z + \frac{2\varepsilon_7-3\varepsilon_8}{\varepsilon_7}t\right) \\ +\Delta_4 \sinh\left(x + \varepsilon_7 y + \varepsilon_8 z + \frac{4\varepsilon_7-3\varepsilon_8}{\varepsilon_7}t\right) \end{bmatrix}} \tag{9}$$

Case 5:

$\varepsilon_1 = \varepsilon_1,\ \varepsilon_2 = \varepsilon_8,\ \varepsilon_3 = \frac{4\varepsilon_1 - 3\varepsilon_8}{\varepsilon_1},\ \varepsilon_4 = -\varepsilon_1,\ \varepsilon_5 = 2\varepsilon_1 - \varepsilon_8,\ \varepsilon_6 = \frac{2\varepsilon_1 - 3\varepsilon_8}{\varepsilon_1},\ \varepsilon_7 = \varepsilon_1,\ \varepsilon_8 = \varepsilon_8,$
$\varepsilon_9 = \frac{4\varepsilon_1 - 3\varepsilon_8}{\varepsilon_1},\ \Delta_1 = \Delta_1,\ \Delta_2 = \Delta_2,\ \Delta_3 = \Delta_3,\ \Delta_4 = \Delta_4.$

Using the above results, we can obtain the multi-wave complexiton solution of Equation (1) via Equation (2) and Equation (5) as:

$$\psi(x,y,z,t)=\frac{2\left[\begin{array}{l}\Delta_1 e^{x+\varepsilon_1 y+\varepsilon_8 z+\frac{4\varepsilon_1-3\varepsilon_8}{\varepsilon_1}t}-\Delta_2 e^{-(x+\varepsilon_1 y+\varepsilon_8 z+\frac{4\varepsilon_1-3\varepsilon_8}{\varepsilon_1}t)}+\Delta_3\cos\left(x-\varepsilon_1 y+\varepsilon_5 z+\frac{2\varepsilon_1-3\varepsilon_8}{\varepsilon_1}t\right)\\ +\Delta_4\cosh\left(x+\varepsilon_1 y+\varepsilon_8 z+\frac{4\varepsilon_1-3\varepsilon_8}{\varepsilon_1}t\right)\end{array}\right]}{\left[\begin{array}{l}\Delta_1 e^{x+\varepsilon_1 y+\varepsilon_8 z+\frac{4\varepsilon_1-3\varepsilon_8}{\varepsilon_1}}+\Delta_2 e^{-(x+\varepsilon_1 y+\varepsilon_8 z+\frac{4\varepsilon_1-3\varepsilon_8}{\varepsilon_1}t)}+\Delta_3\sin\left(x-\varepsilon_1 y+\varepsilon_5 z+\frac{2\varepsilon_1-3\varepsilon_8}{\varepsilon_1}t\right)\\ +\Delta_4\sinh\left(x+\varepsilon_1 y+\varepsilon_8 z+\frac{4\varepsilon_1-3\varepsilon_8}{\varepsilon_1}t\right)\end{array}\right]} \tag{10}$$

Case 6:

$\varepsilon_1=-\varepsilon_4,\ \varepsilon_2=\frac{\varepsilon_4(\varepsilon_9-4)}{3},\ \varepsilon_3=\varepsilon_9,\ \varepsilon_4=\varepsilon_4,\ \varepsilon_5=-\frac{2\varepsilon_4+\varepsilon_4\varepsilon_9}{3},\ \varepsilon_6=\varepsilon_9-2,\ \varepsilon_7=-\varepsilon_4,\ \varepsilon_8=\frac{\varepsilon_4(\varepsilon_9-4)}{3},$
$\varepsilon_9=\varepsilon_9,\ \Delta_1=\Delta_1,\ \Delta_2=\Delta_2,\ \Delta_3=\Delta_3,\ \Delta_4=\Delta_4.$

Putting the above results into Equation (5) and using the transformation of Equation (2), we can obtain the multi-wave complexiton solution as:

$$\psi(x,y,z,t)=\frac{2\left[\begin{array}{l}\Delta_1 e^{x-\varepsilon_4 y+\frac{\varepsilon_4(\varepsilon_9-4)}{3}z+\varepsilon_9 t}-\Delta_2 e^{-(x-\varepsilon_4 y+\frac{\varepsilon_4(\varepsilon_9-4)}{3}z+\varepsilon_9 t)}+\Delta_3\cos\left(x+\varepsilon_4 y-\frac{2\varepsilon_4+\varepsilon_4\varepsilon_9}{3}z+(\varepsilon_9-2)t\right)\\ +\Delta_4\cosh\left(x-\varepsilon_4 y+\frac{\varepsilon_4(\varepsilon_9-4)}{3}z+\varepsilon_9 t\right)\end{array}\right]}{\left[\begin{array}{l}\Delta_1 e^{x-\varepsilon_4 y+\frac{\varepsilon_4(\varepsilon_9-4)}{3}z+\varepsilon_9 t}+\Delta_2 e^{-(x-\varepsilon_4 y+\frac{\varepsilon_4(\varepsilon_9-4)}{3}z+\varepsilon_9 t)}+\Delta_3\sin\left(x+\varepsilon_4 y-\frac{2\varepsilon_4+\varepsilon_4\varepsilon_9}{3}z+(\varepsilon_9-2)t\right)\\ +\Delta_4\sinh\left(x-\varepsilon_4 y+\frac{\varepsilon_4(\varepsilon_9-4)}{3}z+\varepsilon_9 t\right)\end{array}\right]} \tag{11}$$

2.2. The Multi-Wave Solutions

To seek for the multi-wave solutions of Equation (1), we assume that g has the following form:

$$\begin{aligned}\phi&=\varepsilon_1 x+\varepsilon_2 y+\varepsilon_3 z+\varepsilon_4 t+\varepsilon_5,\\ \varphi&=\varepsilon_6 x+\varepsilon_7 y+\varepsilon_8 z+\varepsilon_9 t+\varepsilon_{10},\\ \gamma&=\varepsilon_{11}x+\varepsilon_{12}y+\varepsilon_{13}z+\varepsilon_{14}t+\varepsilon_{15},\\ g&=\Delta_1\cos(\phi)+\Delta_2\cos\mathrm{h}(\varphi)+\Delta_3\cos\mathrm{h}(\gamma)+\varepsilon_{16},\end{aligned} \tag{12}$$

where $\varepsilon_i(i=1,2,\ldots,16)$ and $\Delta_i(i=1,2,3)$ are real parameters to be determined later. Incorporating Equation (12) into Equation (3) yields a set of algebraic equations. Solving them, we have:

Case 1:

$\varepsilon_1=\varepsilon_1,\ \varepsilon_2=0,\ \varepsilon_3=0,\ \varepsilon_4=\varepsilon_4,\ \varepsilon_5=\varepsilon_5,\ \varepsilon_6=\varepsilon_6,\ \varepsilon_7=0,\ \varepsilon_8=0,\ \varepsilon_9=\frac{\varepsilon_6\left(\varepsilon_1^3+\varepsilon_4+\varepsilon_1\varepsilon_6^2\right)}{\varepsilon_1},\ \varepsilon_{10}=\varepsilon_{10},$
$\varepsilon_{11}=0,\ \varepsilon_{12}=\varepsilon_{12},\ \varepsilon_{13}=-\frac{\varepsilon_{12}\left(\varepsilon_1^3+\varepsilon_4\right)}{3\varepsilon_1},\ \varepsilon_{14}=0,$
$\varepsilon_{15}=\varepsilon_{15},\ \varepsilon_{16}=\varepsilon_{16},\ \Delta_1=\Delta_1,\ \Delta_2=\Delta_2,\ \Delta_3=\Delta_3.$

Substituting the above results into Equation (12) and adopting the transformation provided by Equation (2), we can obtain the multi-wave solution as:

$$\psi(x,y,z,t)=\frac{2\left[-\varepsilon_1\Delta_1\sin(\varepsilon_1 x+\varepsilon_4 t+\varepsilon_5)+\varepsilon_6\Delta_2\sin\mathrm{h}\left(\varepsilon_6 x+\frac{\varepsilon_6\left(\varepsilon_1^3+\varepsilon_4+\varepsilon_1\varepsilon_6^2\right)}{\varepsilon_1}t+\varepsilon_{10}\right)\right]}{\begin{array}{l}\Delta_1\cos(\varepsilon_1 x+\varepsilon_4 t+\varepsilon_5)+\Delta_2\cos\mathrm{h}\left(\varepsilon_6 x+\frac{\varepsilon_6\left(\varepsilon_1^3+\varepsilon_4+\varepsilon_1\varepsilon_6^2\right)}{\varepsilon_1}t+\varepsilon_{10}\right)\\ +\Delta_3\cos\mathrm{h}\left(\varepsilon_{12}y-\frac{\varepsilon_{12}\left(\varepsilon_1^3+\varepsilon_4\right)}{3\varepsilon_1}z+\varepsilon_{15}\right)+\varepsilon_{16}\end{array}}. \tag{13}$$

Case 2:

$$\varepsilon_1=\varepsilon_1,\ \varepsilon_2=-\tfrac{\varepsilon_{11}\varepsilon_{12}}{\varepsilon_1},\ \varepsilon_3=\tfrac{\varepsilon_{11}\varepsilon_{12}\left(4\varepsilon_1^3+\varepsilon_4\right)}{3\varepsilon_1^2},\ \varepsilon_4=\varepsilon_4,\ \varepsilon_5=\varepsilon_5,\ \varepsilon_6=\varepsilon_6,\varepsilon_7=\tfrac{\varepsilon_{11}\varepsilon_{12}}{\varepsilon_6},$$
$$\varepsilon_8=-\tfrac{\varepsilon_{11}\varepsilon_{12}\left(\varepsilon_1^3+\varepsilon_4-3\varepsilon_1\varepsilon_6^2\right)}{3\varepsilon_1\varepsilon_6},\ \varepsilon_9=\tfrac{\varepsilon_6\left(\varepsilon_1^3+\varepsilon_4+\varepsilon_1\varepsilon_6^2\right)}{\varepsilon_1},\ \varepsilon_{10}=\varepsilon_{10},\ \varepsilon_{11}=\varepsilon_{11},\ \varepsilon_{12}=\varepsilon_{12},$$
$$\varepsilon_{13}=-\tfrac{\varepsilon_{12}\left(\varepsilon_1^3-3\varepsilon_1\varepsilon_{11}^2+\varepsilon_4\right)}{3\varepsilon_1},\ \varepsilon_{14}=\tfrac{\varepsilon_{11}\left(\varepsilon_1^3+\varepsilon_1\varepsilon_{11}^2+\varepsilon_4\right)}{\varepsilon_1},\ \varepsilon_{15}=\varepsilon_{15},\ \varepsilon_{16}=0,\Delta_1=\Delta_1,\ \Delta_2=\Delta_2,\ \Delta_3=\Delta_3$$

Using the obtained results, we can obtain the multi-wave solution of Equation (1) by Equation (12) and Equation (2) as:

$$\psi(x,y,z,t)=\frac{2\left[\begin{array}{l}-\varepsilon_1\Delta_1\sin\left(\varepsilon_1x-\tfrac{\varepsilon_{11}\varepsilon_{12}}{\varepsilon_1}y+\tfrac{\varepsilon_{11}\varepsilon_{12}\left(4\varepsilon_1^3+\varepsilon_4\right)}{3\varepsilon_1^2}z+\varepsilon_4t+\varepsilon_5\right)\\+\varepsilon_6\Delta_2\sinh\left(\varepsilon_6x+\tfrac{\varepsilon_{11}\varepsilon_{12}}{\varepsilon_6}y-\tfrac{\varepsilon_{11}\varepsilon_{12}\left(\varepsilon_1^3+\varepsilon_4-3\varepsilon_1\varepsilon_6^2\right)}{3\varepsilon_1\varepsilon_6}z+\tfrac{\varepsilon_6\left(\varepsilon_1^3+\varepsilon_4+\varepsilon_1\varepsilon_6^2\right)}{\varepsilon_1}t+\varepsilon_{10}\right)\\+\varepsilon_{11}\Delta_3\sinh\left(\varepsilon_{11}x+\varepsilon_{12}y-\tfrac{\varepsilon_{12}\left(\varepsilon_1^3-3\varepsilon_1\varepsilon_{11}^2+\varepsilon_4\right)}{3\varepsilon_1}z+\tfrac{\varepsilon_{11}\left(\varepsilon_1^3+\varepsilon_1\varepsilon_{11}^2+\varepsilon_4\right)}{\varepsilon_1}t+\varepsilon_{15}\right)\end{array}\right]}{\begin{array}{l}\Delta_1\cos\left(\varepsilon_1x-\tfrac{\varepsilon_{11}\varepsilon_{12}}{\varepsilon_1}y+\tfrac{\varepsilon_{11}\varepsilon_{12}\left(4\varepsilon_1^3+\varepsilon_4\right)}{3\varepsilon_1^2}z+\varepsilon_4t+\varepsilon_5\right)\\+\Delta_2\cosh\left(\varepsilon_6x+\tfrac{\varepsilon_{11}\varepsilon_{12}}{\varepsilon_6}y-\tfrac{\varepsilon_{11}\varepsilon_{12}\left(\varepsilon_1^3+\varepsilon_4-3\varepsilon_1\varepsilon_6^2\right)}{3\varepsilon_1\varepsilon_6}z+\tfrac{\varepsilon_6\left(\varepsilon_1^3+\varepsilon_4+\varepsilon_1\varepsilon_6^2\right)}{\varepsilon_1}t+\varepsilon_{10}\right)\\+\Delta_3\cosh\left(\varepsilon_{11}x+\varepsilon_{12}y-\tfrac{\varepsilon_{12}\left(\varepsilon_1^3-3\varepsilon_1\varepsilon_{11}^2+\varepsilon_4\right)}{3\varepsilon_1}z+\tfrac{\varepsilon_{11}\left(\varepsilon_1^3+\varepsilon_1\varepsilon_{11}^2+\varepsilon_4\right)}{\varepsilon_1}t+\varepsilon_{15}\right)\end{array}} \tag{14}$$

2.3. The Periodic Lump Solutions

To search for the periodic lump solutions of Equation (1). Here, the ansatz function g is supposed as the following form:

$$\phi=x+\varepsilon_1y+\varepsilon_2z+\varepsilon_3t,$$
$$\varphi=x+\varepsilon_4y+\varepsilon_5z+\varepsilon_6t,$$
$$g=\Delta_1\sin(\phi)+\Delta_2\cos\mathrm{h}(\varphi)+\varepsilon_7, \tag{15}$$

where $\varepsilon_i(i=1,2,\ldots,7)$ and $\Delta_i(i=1,2)$ are real parameters that can be determined later. In the same manner, substituting Equation (15) into Equation (3) and performing the corresponding adjustments, we have:

Case 1:

$$\varepsilon_1=-\varepsilon_4,\ \varepsilon_2=\frac{\varepsilon_3+4}{3},\ \varepsilon_3=\varepsilon_3,\ \varepsilon_4=\varepsilon_4,\ \varepsilon_5=\frac{2\varepsilon_4-\varepsilon_3\varepsilon_4}{3},\ \varepsilon_6=\varepsilon_3+2,\ \varepsilon_7=0,\ \Delta_1=\Delta_1,\ \Delta_2=\Delta_2.$$

Substituting the above results into Equation (15) and applying the transformation provided by Equation (2), we can obtain the periodic lump solution of Equation (1) as:

$$\psi(x,y,z,t)=\frac{2\left[\Delta_1\cos\left(x-\varepsilon_4y+\tfrac{\varepsilon_3+4}{3}z+\varepsilon_3t\right)+\Delta_2\sin\mathrm{h}\left(x+\varepsilon_4y+\tfrac{2\varepsilon_4-\varepsilon_3\varepsilon_4}{3}z+(\varepsilon_3+2)t\right)\right]}{\Delta_1\sin\left(x-\varepsilon_4y+\tfrac{\varepsilon_3+4}{3}z+\varepsilon_3t\right)+\Delta_2\cos\mathrm{h}\left(x+\varepsilon_4y+\tfrac{2\varepsilon_4-\varepsilon_3\varepsilon_4}{3}z+(\varepsilon_3+2)t\right)}. \tag{16}$$

Case 2:

$$\varepsilon_1=\varepsilon_1,\ \varepsilon_2=-\frac{2\varepsilon_1+\varepsilon_1\varepsilon_6}{3},\ \varepsilon_3=\varepsilon_6-2,\ \varepsilon_4=-\varepsilon_1,\ \varepsilon_5=\frac{\varepsilon_1\varepsilon_6-4\varepsilon_1}{3},\ \varepsilon_6=\varepsilon_6,\ \varepsilon_7=0,\ \Delta_1=\Delta_1,\ \Delta_2=\Delta_2.$$

Bringing the obtained results into Equation (15), we can obtain the periodic lump solution of Equation (1) with the help of the transformation provided by Equation (2) as:

$$\psi(x,y,z,t)=\frac{2\left[\Delta_1\cos\left(x+\varepsilon_1y-\tfrac{2\varepsilon_1+\varepsilon_1\varepsilon_6}{3}z+(\varepsilon_6-2)t\right)+\Delta_2\sin\mathrm{h}\left(x-\varepsilon_1y+\tfrac{\varepsilon_1\varepsilon_6-4\varepsilon_1}{3}z+\varepsilon_6t\right)\right]}{\Delta_1\sin\left(x+\varepsilon_1y-\tfrac{2\varepsilon_1+\varepsilon_1\varepsilon_6}{3}z+(\varepsilon_6-2)t\right)+\Delta_2\cos\mathrm{h}\left(x-\varepsilon_1y+\tfrac{\varepsilon_1\varepsilon_6-4\varepsilon_1}{3}z+\varepsilon_6t\right)}. \tag{17}$$

3. The Traveling Wave Solutions

In this section, we will inquire into the traveling wave solutions of Equation (1) with the aid of the sub-equation method [47,48].

To obtain the traveling wave solutions, we first introduce the following variable transformation:

$$\psi(x,y,z,t) = \Psi(\zeta),\ \zeta = mx + ny + kz + st, \tag{18}$$

where m, n, k, s are non-zero constants. Putting it into Equation (1) yields:

$$m^3 n\Psi^{(4)} + 3m^2 n\left[(\Psi')^2\right]' - (ns + 3mk)\Psi'' = 0, \tag{19}$$

Integrating Equation (19) with respect to ζ once and ignoring the integral constant, we have:

$$m^3 n\Psi''' + 3m^2 n(\Psi')^2 - (ns + 3mk)\Psi' = 0, \tag{20}$$

Using the sub-equation method, we can assume the solution of Equation (20) is:

$$\Psi(\zeta) = \sum_{i=0}^{c} \alpha_i \Re^i(\zeta). \tag{21}$$

where $\alpha_i (i = 0, 1, 2. \ldots,\ c)$ are constants that can be determined later. Additionally, there is:

$$\Re'(\zeta) = \mu + \Re^2(\gamma). \tag{22}$$

Here, μ is a constant. The solutions of Equation (22) are:

$$\Re(\zeta) = \begin{cases} -\sqrt{-\mu}\tan\text{h}(\sqrt{-\mu}\zeta), & \mu < 0 \\ -\sqrt{-\mu}\cot\text{h}(\sqrt{-\mu}\zeta), & \mu < 0 \\ \sqrt{\mu}\tan(\sqrt{\mu}\zeta), & \mu > 0 \\ -\sqrt{\mu}\cot(\sqrt{\mu}\zeta), & \mu > 0 \\ -\frac{1}{\zeta+\Lambda},\ \Lambda\ \ is\ \ a\ \ \text{constant}, & \mu = 0 \end{cases}. \tag{23}$$

By balancing Ψ''' and $(\Psi')^2$ in Equation (20), the value of c in Equation (21) can be determined as:

$$c = 1. \tag{24}$$

Thus, we have:

$$\Psi(\zeta) = \alpha_0 + \alpha_1 \Re(\zeta). \tag{25}$$

Now, substituting Equation (25) with Equation (22) into Equation (20) and setting their coefficients of the different powers of $\Re(\zeta)$ to be zero yields:

$\Re^0(\zeta)$: $-3km\mu\alpha_1 - ns\mu\alpha_1 + 2m^3 n\mu^2\alpha_1 + 3m^2 n\mu^2\alpha_1^2 = 0$,
$\Re^2(\zeta)$: $-3km\alpha_1 - ns\alpha_1 + 8m^3 n\mu\alpha_1 + 6m^2 n\mu\alpha_1^2 = 0$,
$\Re^4(\zeta)$: $6m^3 n\alpha_1 + 3m^2 n\alpha_1^2 = 0$.

On solving them, we have:

Case 1:

$$\alpha_0 = \alpha_0,\ \alpha_1 = \alpha_1,\ m = -\frac{\alpha_1}{2},\ n = n,\ k = k,\ s = \frac{\alpha_1(3k + n\mu\alpha_1^2)}{2n},\ \mu = \mu.$$

So, the traveling wave solutions of Equation (1) can be obtained as:

$$\psi(x,y,z,t) = \alpha_0 - \alpha_1\sqrt{-\mu}\tan\text{h}\left[\sqrt{-\mu}\left(-\frac{\alpha_1}{2}x + ny + kz + \frac{\alpha_1(3k + n\mu\alpha_1^2)}{2n}t\right)\right],\ \mu < 0 \tag{26}$$

$$\psi(x,y,z,t) = \alpha_0 - \alpha_1\sqrt{-\mu}\cot\text{h}\left[\sqrt{-\mu}\left(-\frac{\alpha_1}{2}x + ny + kz + \frac{\alpha_1(3k + n\mu\alpha_1^2)}{2n}t\right)\right],\ \mu < 0 \tag{27}$$

$$\psi(x,y,z,t) = \alpha_0 + \alpha_1\sqrt{\mu}\tan\left[\sqrt{\mu}\left(-\frac{\alpha_1}{2}x + ny + kz + \frac{\alpha_1\left(3k + n\mu\alpha_1^2\right)}{2n}t\right)\right],\ \mu > 0 \tag{28}$$

$$\psi(x,y,z,t) = \alpha_0 - \alpha_1\sqrt{\mu}\cot\left[\sqrt{\mu}\left(-\frac{\alpha_1}{2}x + ny + kz + \frac{\alpha_1\left(3k + n\mu\alpha_1^2\right)}{2n}t\right)\right],\ \mu > 0 \tag{29}$$

Case 2:

$$\alpha_0 = \alpha_0,\ \alpha_1 = -2m,\ m = m,\ n = n,\ k = -\frac{ns + 4m^3n\mu}{3m},\ s = s,\ \mu = \mu.$$

So, the traveling wave solutions of Equation (1) can be obtained as:

$$\psi(x,y,z,t) = \alpha_0 + 2m\sqrt{-\mu}\tanh\left[\sqrt{-\mu}\left(mx + ny - \frac{ns + 4m^3n\mu}{3m}z + st\right)\right] \tag{30}$$

$$\psi(x,y,z,t) = \alpha_0 + 2m\sqrt{-\mu}\coth\left[\sqrt{-\mu}\left(mx + ny - \frac{ns + 4m^3n\mu}{3m}z + st\right)\right],\ \mu < 0. \tag{31}$$

$$\psi(x,y,z,t) = \alpha_0 - 2m\sqrt{\mu}\tan\left[\sqrt{\mu}\left(mx + ny - \frac{ns + 4m^3n\mu}{3m}z + st\right)\right],\ \mu > 0. \tag{32}$$

$$\psi(x,y,z,t) = \alpha_0 + 2m\sqrt{\mu}\cot\left[\sqrt{\mu}\left(mx + ny - \frac{ns + 4m^3n\mu}{3m}z + st\right)\right] \tag{33}$$

4. The Numerical Results and Physical Interpretations

The numerical results will be presented by the 3-D plots, 2-D contours, and 2-D curves in this section by assigning the reasonable parameters with the help of the Mathematica software.

Figure 1 presents the behavior of the multi-waves complexiton solution provided by Equation (6) for using $\varepsilon_2 = 2$, $\varepsilon_9 = 3$, $\Delta_1 = 1$, $\Delta_2 = -1$, $\Delta_3 = 1$, $\Delta_4 = 1$ for $z = 0$ at $t = 0$, $t = 4$ and $t = 8$ in the form of a 3-D plot and 2-D contour. It can be observed that there were collision phenomena between the lump and singular periodic waves arising in the outline. As the time goes on, the wave is propagating along the negative direction of the x-axis and y-axis.

By assigning the parameters as $\varepsilon_1 = 1$, $\varepsilon_4 = 1$, $\varepsilon_5 = 1$, $\varepsilon_6 = 1$, $\varepsilon_{10} = 1$, $\varepsilon_{12} = 1$, $\varepsilon_{15} = 1$, $\varepsilon_{16} = 1$, $\Delta_1 = 1$, $\Delta_2 = 1$, and $\Delta_3 = 1$, we present the performance of Equation (13) in Figure 2 for $z = 0$ at $t = 0$, $t = 2$, and $t = 4$ through the 3-D plots and 2-D contours. We can find that the multi-wave is formed by the interleaving and superposition of two waveforms. As time goes on, one wave is propagating along the negative direction of x-axis and positive direction of y-axis, on the other hand, the other wave is propagating along the negative direction of the x-axis and y-axis.

Figure 3 presents the behaviors of Equation (16) by selecting the parameters as $\varepsilon_3 = 1$, $\varepsilon_4 = 1$, $\Delta_1 = 1$, and $\Delta_2 = 1$ at $z = 1$ for $t = 0$, $t = 1$, and $t = 2$ via the 3-D plots and 2-D contours. It is easy to see the collision phenomena between the lump and singular periodic waves arising in the outline. With the increase in t, the waveform propagates along the negative direction of the x-axis and y-axis.

Assigning the parameters as $\alpha_0 = 1$, $\alpha_1 = 1$, $n = 1$, $k = 1$, and $\mu = -1$, the behaviors of Equation (26) and Equation (27) are described in Figures 4 and 5, respectively. We can find the waveform of Equation (26) is the dark wave and of Equation (27) is the bright-dark wave.

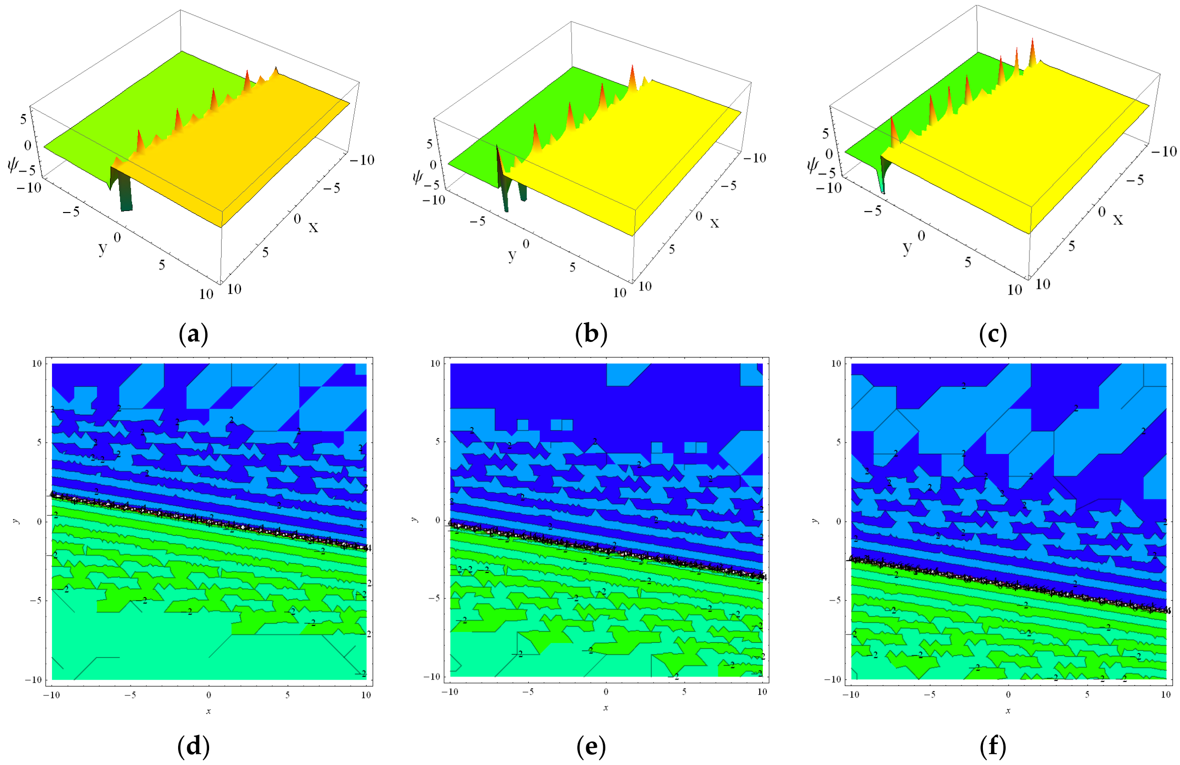

Figure 1. The 3-D plots and 2-D contours of Equation (6) with the parameters as $\varepsilon_2 = 2$, $\varepsilon_9 = 3$, $\Delta_1 = 1$, $\Delta_2 = -1$, $\Delta_3 = 1$, and $\Delta_4 = 1$ at $z = 0$. (**a**,**d**) for $t = 0$, (**b**,**e**) for $t = 4$, (**c**,**f**), and for $t = 8$.

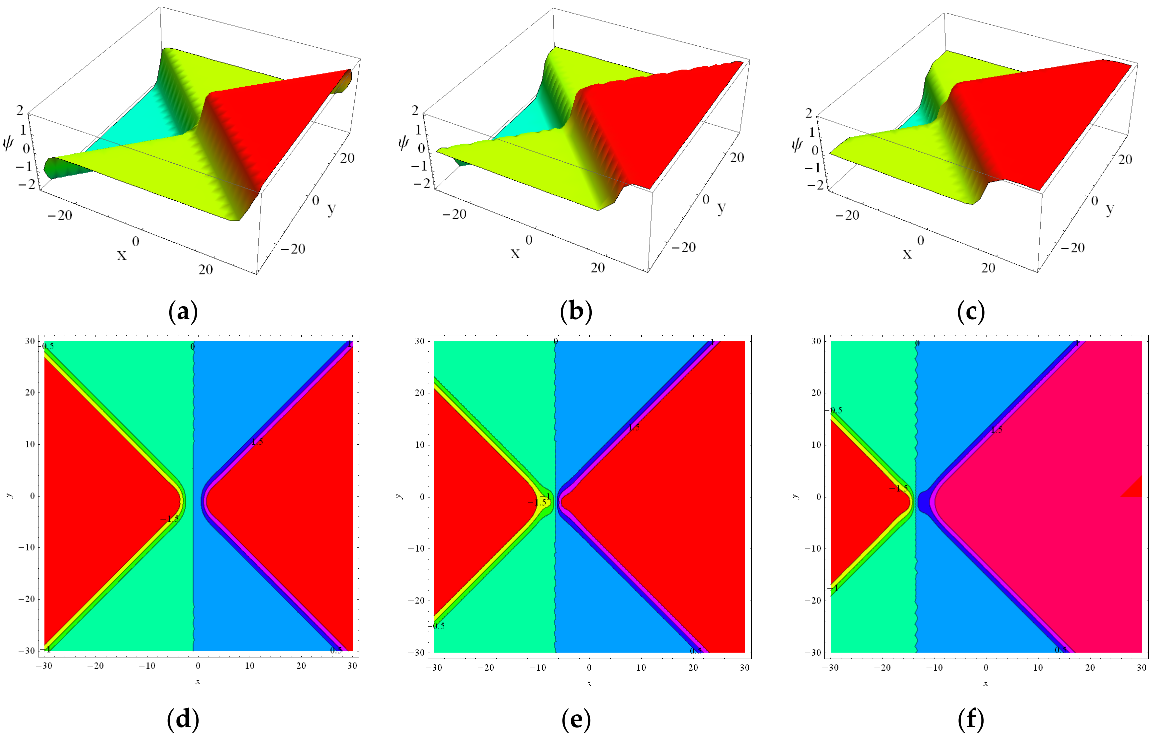

Figure 2. The 3-D plots and 2-D contours of Equation (13) with the parameters as $\varepsilon_1 = 1$, $\varepsilon_4 = 1$, $\varepsilon_5 = 1$, $\varepsilon_6 = 1$, $\varepsilon_{10} = 1$, $\varepsilon_{12} = 1$, $\varepsilon_{15} = 1$, $\varepsilon_{16} = 1$, $\Delta_1 = 1$, $\Delta_2 = 1$, and $\Delta_3 = 1$ at $z = 0$. (**a**,**d**) for $t = 0$, (**b**,**e**) for $t = 2$, and (**c**,**f**) for $t = 4$.

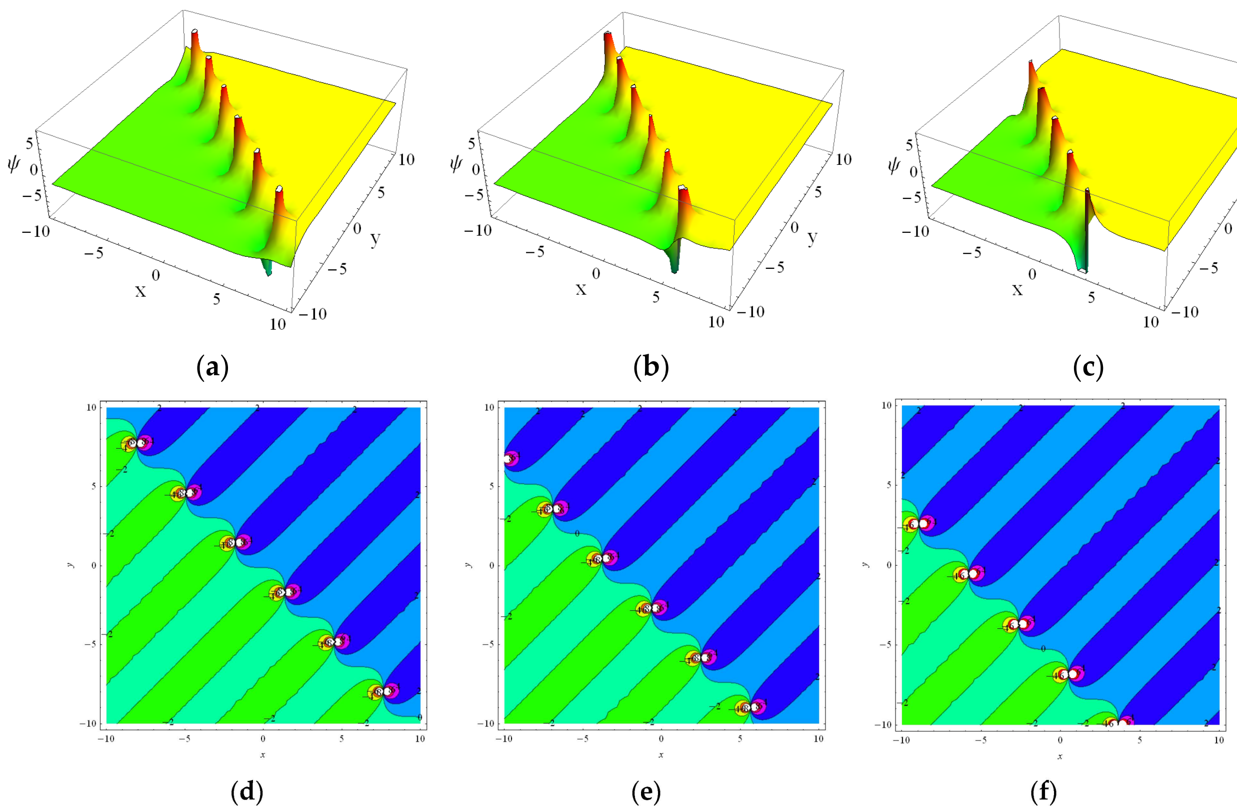

Figure 3. The 3-D plots and 2-D contours of Equation (16) with the parameters as $\varepsilon_3 = 1$, $\varepsilon_4 = 1$, $\Delta_1 = 1$, and $\Delta_2 = 1$ at $z = 1$. (**a**,**d**) for $t = 0$, (**b**,**e**) for $t = 1$, and (**c**,**f**) for $t = 2$.

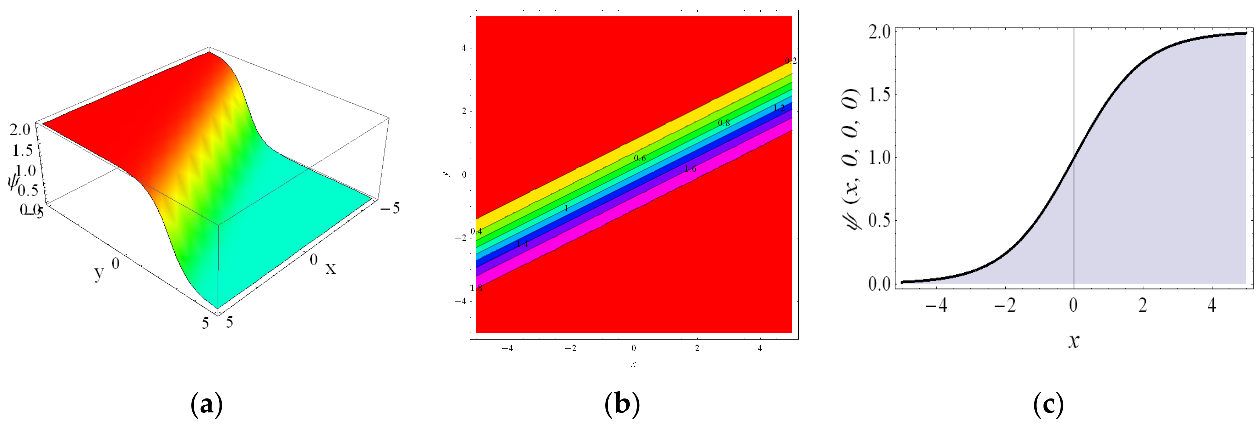

Figure 4. The 3-D plots and 2-D curve of Equation (26) with the parameters as $\alpha_0 = 1$, $\alpha_1 = 1$, $n = 1$, $k = 1$, and $\mu = -1$. (**a**) 3-D plot for $z = 0$ and $t = 0$, (**b**) 2-D contour for $z = 0$ and $t = 0$, and (**c**) 2-D curve for $y = 0$, $z = 0$, and $t = 0$.

If we choose the parameters as $\alpha_0 = 1$, $m = 1$, $n = 1$, $s = 1$, and $\mu = 1$, we present the performances of Equation (28) and Equation (29) in Figures 6 and 7, respectively. It can be observed that the profiles are both the singular periodic waves.

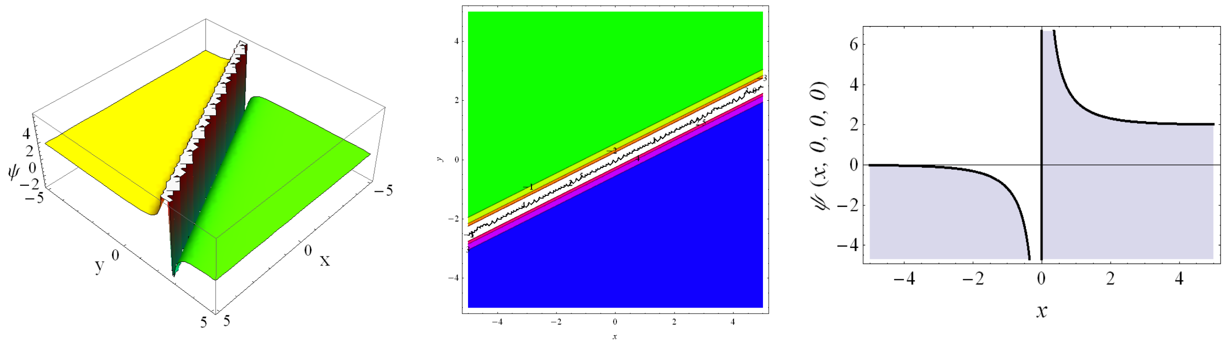

(**a**) (**b**) (**c**)

Figure 5. The 3-D plots and 2-D curve of Equation (27) with the parameters as $\alpha_0 = 1$, $\alpha_1 = 1$, $n = 1$, $k = 1$, and $\mu = -1$. (**a**) 3-D plot for $z = 0$ and $t = 0$, (**b**) 2-D contour for $z = 0$ and $t = 0$, and (**c**) 2-D curve for $y = 0$, $z = 0$, and $t = 0$.

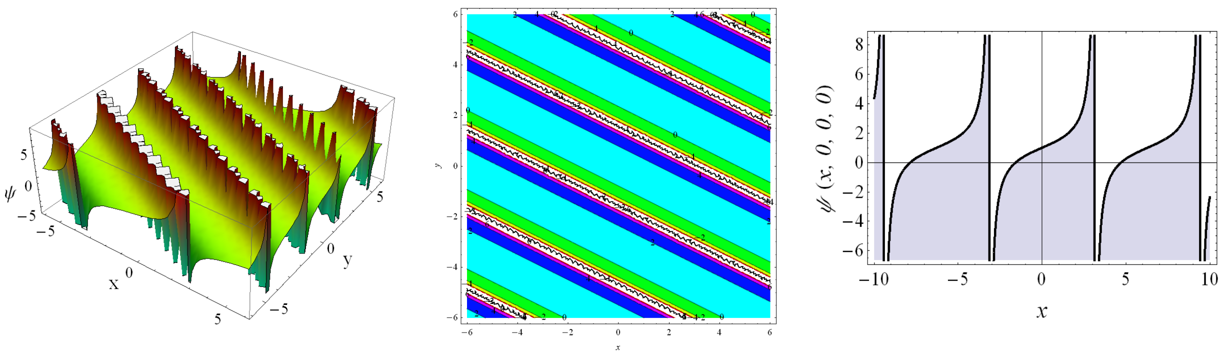

(**a**) (**b**) (**c**)

Figure 6. The 3-D plots and 2-D contours of Equation (28) with the parameters as $\alpha_0 = 1$, $\alpha_1 = 1$, $n = 1$, $k = 1$, and $\mu = 1$. (**a**) 3-D plot for $z = 0$ and $t = 0$, (**b**) 2-D contour for $z = 0$ and $t = 0$, and (**c**) 2-D curve for $y = 0$, $z = 0$, and $t = 0$.

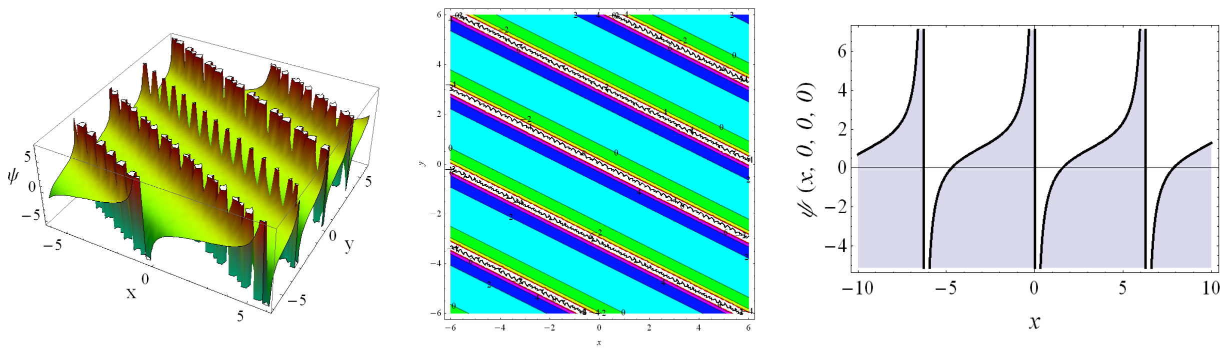

(**a**) (**b**) (**c**)

Figure 7. The 3-D plots and 2-D contours of Equation (29) with the parameters as $\alpha_0 = 1$, $m = 1$, $n = 1$, $s = 1$, and $\mu = 1$. (**a**) 3-D plot for $z = 0$ and $t = 0$, (**b**) 2-D contour for $z = 0$ and $t = 0$, (**c**) 2-D curve for $y = 0$, $z = 0$, and $t = 0$.

5. Conclusions and Future Recommendations

With the aid of the Cole—Hopf transform, we successfully constructed the multi-wave complexiton, multi-wave, and periodic-lump solutions of the (3+1)-dimensional B-type Kadomtsev—Petviashvili equation via applying the symbolic computation and the ansatz function schemes. Furthermore, we also find its abundant exact traveling solutions by means of the sub-equation method, which includes the dark wave, bright-dark wave, and singular periodic wave solutions. Finally, the numerical simulation of the solutions are presented through the 3-D plots, 2-D contours, and 2-D curves. Compared with the solutions reported in [35–40], it can be found that the diverse solutions in this work are all new, which can be used to extend the solutions of the (3+1)-dimensional B-type Kadomtsev—Petviashvili equation in fluid mechanics. The methods in this paper can be applied to study the exact solutions of the other PDEs in physics.

Recently, the fractal and fractional calculus have a wide range of applications in different fields [49–57]; how to apply them to Equation (1) is the direction of the future research.

Author Contributions: Conceptualization, K.-J.W.; methodology, K.-J.W.; writing—original draft preparation, K.-J.W.; writing—review and editing, J.-H.L.; data curation, J.S.; supervision, G.-D.W. All authors have read and agreed to the published version of the manuscript.

Funding: This work is supported by the Key Programs of Universities in Henan Province of China (22A140006), the Fundamental Research Funds for the Universities of Henan Province (NSFRF210324), Program of Henan Polytechnic University (B2018-40), the Innovative Scientists and Technicians Team of Henan Provincial High Education (21IRTSTHN016).

Data Availability Statement: The data that support the findings of this study are available from the corresponding author upon reasonable request.

Conflicts of Interest: The authors declare no conflict of interest.

References

1. Jhangeer, A.; Hussain, A.; Junaid-U-Rehman, M.; Baleanu, D.; Riaz, M.B. Quasi-periodic, chaotic and travelling wave structures of modified Gardner equation. *Chaos Solitons Fractals* **2021**, *143*, 110578. [CrossRef]
2. Wang, K.L. New perspective to the fractal Konopelchenko-Dubrovsky equations with M-truncated fractional derivative. *Int. J. Geom. Methods Mod. Phys.* **2023**, *2023*, 2350072. [CrossRef]
3. Wang, K.J.; Si, J. On the non-differentiable exact solutions of the (2+1)-dimensional local fractional breaking soliton equation on Cantor sets. *Math. Methods Appl. Sci.* **2023**, *46*, 1456–1465. [CrossRef]
4. Wang, K.L. Exact travelling wave solution for the local fractional Camassa-Holm-Kadomtsev-Petviashvili equation. *Alex. Eng. J.* **2022**, *63*, 371–376. [CrossRef]
5. Yang, Z.; Cheng, D.; Cong, G.; Jin, D.; Borjalilou, V. Dual-phase-lag thermoelastic damping in nonlocal rectangular nanoplates. *Waves Random Complex Media* **2021**, 1–20. [CrossRef]
6. Wang, K.J.; Jing, S. Dynamic properties of the attachment oscillator arising in the nanophysics. *Open Phys.* **2023**. [CrossRef]
7. Ma, Y.X.; Tian, B.; Qu, Q.X.; Yang, D.-Y.; Chen, Y.-Q. Painlevé analysis, Bäcklund transformations and traveling-wave solutions for a (3+1)-dimensional generalized Kadomtsev-Petviashvili equation in a fluid. *Int. J. Mod. Phys. B* **2021**, *35*, 2150108. [CrossRef]
8. Yin, Y.H.; Lü, X.; Ma, W.X. Bäcklund transformation, exact solutions and diverse interaction phenomena to a (3+1)-dimensional nonlinear evolution equation. *Nonlinear Dyn.* **2022**, *108*, 4181–4194. [CrossRef]
9. Wang, K.J. Bäcklund transformation and diverse exact explicit solutions of the fractal combined KdV-mKdV equation. *Fractals* **2022**, *30*, 2250189. [CrossRef]
10. Du, Z.; Tian, B.; Xie, X.Y.; Jun, C.; Wu, X.Y. Bäcklund transformation and soliton solutions in terms of the Wronskian for the Kadomtsev–Petviashvili-based system in fluid dynamics. *Pramana* **2018**, *90*, 45. [CrossRef]
11. Ma, W.X. Lump solutions to the Kadomtsev-Petviashvili equation. *Phys. Lett. A* **2015**, *379*, 1975–1978. [CrossRef]
12. Wang, K.J.; Liu, J.-H. Diverse optical soliton solutions to the Kundu-Mukherjee-Naskar equation via two novel techniques. *Optik* **2023**, *273*, 170403. [CrossRef]
13. Wang, K.J. Diverse soliton solutions to the Fokas system via the Cole-Hopf transformation. *Optik* **2023**, *272*, 170250. [CrossRef]
14. Zhang, Z.; Li, B.; Chen, J.; Guo, Q. Construction of higher-order smooth positons and breather positons via Hirota's bilinear method. *Nonlinear Dyn.* **2021**, *105*, 2611–2618. [CrossRef]
15. Wang, K.J. Variational principle and diverse wave structures of the modified Benjamin-Bona-Mahony equation arising in the optical illusions field. *Axioms* **2022**, *11*, 445. [CrossRef]
16. Wang, K.J.; Shi, F.; Wang, G.D. Periodic wave structure of the fractal generalized fourth order Boussinesq equation travelling along the non-smooth boundary. *Fractals* **2022**, *30*, 2250168. [CrossRef]
17. Mahak, N.; Akram, G. Extension of rational sine-cosine and rational sinh-cosh techniques to extract solutions for the perturbed NLSE with Kerr law nonlinearity. *Eur. Phys. J. Plus* **2019**, *134*, 1–10. [CrossRef]
18. Wang, K.J.; Liu, J.-H.; Wu, J. Soliton solutions to the Fokas system arising in monomode optical fibers. *Optik* **2022**, *251*, 168319. [CrossRef]
19. Rezazadeh, H.; Inc, M.; Baleanu, D. New solitary wave solutions for variants of (3+1)-dimensional Wazwaz-Benjamin-Bona-Mahony equations. *Front. Phys.* **2020**, *8*, 332. [CrossRef]

20. Wang, K.J.; Liu, J.H. On abundant wave structures of the unsteady korteweg-de vries equation arising in shallow water. *J. Ocean. Eng. Sci.* **2022**, *in press*. [CrossRef]
21. Kudryashov, N.A. One method for finding exact solutions of nonlinear differential equations. *Commun. Nonlinear Sci. Numer. Simul.* **2012**, *17*, 2248–2253. [CrossRef]
22. Alharbi, A.R.; Almatrafi, M.B.; Seadawy, A.R. Construction of the numerical and analytical wave solutions of the Joseph-Egri dynamical equation for the long waves in nonlinear dispersive systems. *Int. J. Mod. Phys. B* **2020**, *34*, 2050289. [CrossRef]
23. Seadawy, A.R.; Kumar, D.; Chakrabarty, A.K. Dispersive optical soliton solutions for the hyperbolic and cubic-quintic nonlinear Schrödinger equations via the extended sinh-Gordon equation expansion method. *Eur. Phys. J. Plus* **2018**, *133*, 182. [CrossRef]
24. Raza, N.; Arshed, S.; Sial, S. Optical solitons for coupled Fokas-Lenells equation in birefringence fibers. *Mod. Phys. Lett. B* **2019**, *33*, 1950317. [CrossRef]
25. Afzal, U.; Raza, N.; Murtaza, I.G. On soliton solutions of time fractional form of Sawada-Kotera equation. *Nonlinear Dyn.* **2019**, *95*, 391–405. [CrossRef]
26. Raza, N.; Javid, A. Optical dark and dark-singular soliton solutions of (1+ 2)-dimensional chiral nonlinear Schrodinger's equation. *Waves Random Complex Media* **2019**, *29*, 496–508. [CrossRef]
27. Wang, K.J.; Si, J. Optical solitons to the Radhakrishnan-Kundu-Lakshmanan equation by two effective approaches. *Eur. Phys. J. Plus* **2022**, *137*, 1016. [CrossRef]
28. Zheng, B.; Wen, C. Exact solutions for fractional partial differential equations by a new fractional sub-equation method. *Adv. Differ. Equ.* **2013**, *2013*, 199. [CrossRef]
29. Wang, K.J. A fractal modification of the unsteady korteweg-de vries model and its generalized fractal variational principle and diverse exact solutions. *Fractals* **2022**, *30*, 2250192. [CrossRef]
30. Wang, K.J. A fast insight into the optical solitons of the generalized third-order nonlinear Schrödinger's equation. *Results Phys.* **2022**, *40*, 105872. [CrossRef]
31. Sağlam Özkan, Y.; Seadawy, A.R.; Yaşar, E. Multi-wave, breather and interaction solutions to (3+1) dimensional Vakhnenko-Parkes equation arising at propagation of high-frequency waves in a relaxing medium. *J. Taibah Univ. Sci.* **2021**, *15*, 666–678. [CrossRef]
32. Seadawy, A.R.; Bilal, M.; Younis, M.; Rizvi, S.T.R.; Althobaiti, S.; Makhlouf, M.M. Analytical mathematical approaches for the double-chain model of DNA by a novel computational technique. *Chaos Solitons Fractals* **2021**, *144*, 110669. [CrossRef]
33. Mohammed, W.W.; Albalahi, A.M.; Albadrani, S.; Aly, E.S.; Sidaoui, R.; Matouk, A.E. The Analytical Solutions of the Stochastic Fractional Kuramoto-Sivashinsky Equation by Using the Riccati Equation Method. *Math. Probl. Eng.* **2022**, *2022*, 5083784. [CrossRef]
34. Al-Askar, F.M.; Mohammed, W.W.; Alshammari, M. Impact of brownian motion on the analytical solutions of the space-fractional stochastic approximate long water wave equation. *Symmetry* **2022**, *14*, 740. [CrossRef]
35. Rizvi, S.T.R.; Seadawy, A.R.; Ali, I.; Bibi, I.; Younis, M. Chirp-free optical dromions for the presence of higher order spatio-temporal dispersions and absence of self-phase modulation in birefringent fibers. *Mod. Phys. Lett. B* **2020**, *34*, 2050399. [CrossRef]
36. Ding, C.C.; Gao, Y.T.; Deng, G.F. Breather and hybrid solutions for a generalized (3+1)-dimensional B-type Kadomtsev-Petviashvili equation for the water waves. *Nonlinear Dyn.* **2019**, *97*, 2023–2040. [CrossRef]
37. Abudiab, M.; Khalique, C.M. Exact solutions and conservation laws of a (3+ 1)-dimensional B-type Kadomtsev-Petviashvili equation. *Adv. Differ. Equ.* **2013**, *2013*, 1–7. [CrossRef]
38. Huang, Z.R.; Tian, B.; Zhen, H.L.; Jiang, Y.; Wang, Y.P.; Sun, Y. Bäcklund transformations and soliton solutions for a (3+1)-dimensional B-type Kadomtsev-Petviashvili equation in fluid dynamics. *Nonlinear Dyn.* **2015**, *80*, 1–7. [CrossRef]
39. Xu, Z.; Chen, H.; Dai, Z. Kink degeneracy and rogue potential solution for the (3+1)-dimensional B-type Kadomtsev-Petviashvili equation. *Pramana* **2016**, *87*, 31. [CrossRef]
40. Cui, W.; Liu, Y.; Li, Z. Multiwave interaction solutions for a (3+1)-dimensional B-type Kadomtsev-Petviashvili equation in fluid dynamics. *Int. J. Nonlinear Sci. Numer. Simul.* **2021**. [CrossRef]
41. Ma, H.; Huang, H.; Deng, A. Soliton molecules and some novel hybrid solutions for (3+1)-dimensional B-type Kadomtsev-Petviashvili equation. *Mod. Phys. Lett. B* **2021**, *35*, 2150388. [CrossRef]
42. Darvishi, M.T.; Najafi, M.; Arbabi, S.; Kavitha, L. Exact propagating multi-anti-kink soliton solutions of a (3+1)-dimensional B-type Kadomtsev-Petviashvili equation. *Nonlinear Dyn.* **2016**, *83*, 1453–1462. [CrossRef]
43. Liu, J.G.; Zhu, W.H.; Osman, M.S.; Ma, W.-X. An explicit plethora of different classes of interactive lump solutions for an extension form of 3D-Jimbo-Miwa model. *Eur. Phys. J. Plus* **2020**, *135*, 412. [CrossRef]
44. Lü, X.; Chen, S.-J. Interaction solutions to nonlinear partial differential equations via Hirota bilinear forms: One-lump-multi-stripe and one-lump-multi-soliton types. *Nonlinear Dyn.* **2021**, *103*, 947–977. [CrossRef]
45. Lü, X.; Chen, S.-J. New general interaction solutions to the KPI equation via an optional decoupling condition approach. *Commun. Nonlinear Sci. Numer. Simul.* **2021**, *103*, 105939. [CrossRef]
46. Ma, W.X. N-soliton solution and the Hirota condition of a (2+1)-dimensional combined equation. *Math. Comput. Simul.* **2021**, *190*, 270–279. [CrossRef]
47. Akinyemi, L.; Şenol, M.; Iyiola, O.S. Exact solutions of the generalized multidimensional mathematical physics models via sub-equation method. *Math. Comput. Simul.* **2021**, *182*, 211–233. [CrossRef]
48. Bekir, A.; Aksoy, E.; Cevikel, A.C. Exact solutions of nonlinear time fractional partial differential equations by sub-equation method. *Math. Methods Appl. Sci.* **2015**, *38*, 2779–2784. [CrossRef]

49. Wang, K.J.; Liu, J.H. Periodic solution of the time-space fractional Sasa-Satsuma equation in the monomode optical fibers by the energy balance theory. *EPL* **2022**, *138*, 25002. [CrossRef]
50. He, J.H.; He, C.H.; Saeed, T. A fractal modification of Chen-Lee-Liu equation and its fractal variational principle. *Int. J. Mod. Phys. B* **2021**, *35*, 2150214. [CrossRef]
51. Wang, K.J.; Liu, J.H.; Si, J.; Shi, F. A new perspective on the exact solutions of the local fractional modified Benjamin-Bona-Mahony equation on Cantor sets. *Fractal Fract.* **2023**, *7*, 72. [CrossRef]
52. He, J.H. Fractal calculus and its geometrical explanation. *Results Phys.* **2018**, *10*, 272–276. [CrossRef]
53. Wang, K.J.; Zhu, H.W. Periodic wave solution of the Kundu-Mukherjee-Naskar equation in birefringent fibers via the Hamiltonian-based algorithm. *EPL* **2022**, *139*, 35002. [CrossRef]
54. Yang, X.J.; Machado, J.A.T.; Cattani, C.; Gao, F. On a fractal LC-electric circuit modeled by local fract, On a fractal LC electric circuit modeled by local fractional calculus. *Commun. Nonlinear Sci. Numer. Simul.* **2017**, *47*, 200–206. [CrossRef]
55. Wang, K.L. A novel variational approach to fractal Swift-Hohenberg model arising in fluid dynamics. *Fractals* **2022**, *30*, 2250156. [CrossRef]
56. Baleanu, D.; Mohammadi, H.; Rezapour, S. Analysis of the model of HIV-1 infection of CD4+ T-cell with a new approach of fractional derivative. *Adv. Differ. Equ.* **2020**, *2020*, 71. [CrossRef]
57. Wang, K.J. Exact traveling wave solutions to the local fractional (3+1)-dimensional Jimbo-Miwa equation on Cantor sets. *Fractals* **2022**, *30*, 2250102. [CrossRef]